Early Motor Pattern Analysis Using a Single RGB-D Camera: A Case Study of Twins at Divergent Risk for Motor Impairment

Early Motor Pattern Analysis Using a Single RGB-D Camera: A Case Study of Twins at Divergent Risk for Motor Impairment

D. Balta, I. G. Porco, H. Hoang, A. Cereatti, P. S. Lum, U. Della Croce, and M. M. Schladen

***Abstract*—Early identification of motor impairment in infants at developmental risk can benefit from objective assessment methods. In this feasibility study, we evaluated quantitative kinematic metrics extracted from home-based recordings as indicators of developmental differences between twins with divergent perinatal outcomes. Two 4-month-old twins, one typically developing and one at-risk of motor impairment, were recorded using a single RGB-D camera at home. Videos of up to three minutes per twin were captured at seven timepoints, about 30 days apart. Seven upper body points of interest were tracked using DeepLabCut and their 3D coordinates calculated with an improved version of a previously published method adapted for home use. Thirteen metrics were estimated at each timepoint. Most metrics were consistent with the trends reported in the literature, distinguishing divergent perinatal outcomes. These findings demonstrated that the proposed method is usable for home-based data collection, compensating for motion artifacts and reducing manual labeling time.**

***Index Terms*—Perinatal brain injury, general movements, markerless, RGB-D, twins.**

***Impact Statement*—This case study on a pair of twins demonstrated that the methodology employed can extract metrics potentially useful for early identification of movement disorders.**

I. Introduction

PERINATAL neurologic injury can disrupt typical motor development, with functional consequences that evolve over the first years of life [1]. Because neuroplasticity is greatest in early infancy, this period represents a critical window for activity-based intervention [2], [3]. The most prevalent condition arising from neuromotor perinatal injury is cerebral palsy (CP), affecting approximately 11 in 1,000 births [4].

CP is usually diagnosed between 12–24 months of age, when motor impairments become clinically evident, yet optimal therapeutic benefit occurs in the first months of life [5]. This gap creates a clinical need for early identification tools capable of detecting infants at risk before conclusive diagnosis. Consequently, we use the terminology "typically developing" (TD) and "at-risk" (AR) rather than clinical diagnostic labels, recognizing that our assessment targets the pre-diagnostic period when early intervention is most beneficial [6], [7], [8].

Recent clinical consensus has highlighted significant uncertainties in applying the traditional CP diagnostic definition, particularly regarding age cutoffs and interpretation of nonprogressive clinical phenotypes [9]. Modern best practice recommends ‘high-risk CP’ terminology for infants under two years when standardized assessments suggest motor impairment, but definitive diagnosis is premature [10], and promotes descriptive clinical characterization over strict radiographic categorization [11]. This evolving perspective reinforces our focus on kinematic movement analysis in twins with differential perinatal brain injury rather than on CP prediction.

Various research explored video-based quantification of spontaneous movements in infants at risk of CP [12], [13], [14] often extracting kinematic or frequency-domain features to train classifiers (e.g., [15], [16]).

A major clinical reference remains the General Movements Assessment (GMA), which evaluates spontaneous movements quality as an indicator of neurological impairment [17], [18]. Although a potent predictor of CP, the GMA is limited to a narrow age range (3–5 months), requires controlled conditions, and demands specialized training, restricting its use in community practice [19].

Nevertheless, GMA remains the clinical gold standard and has inspired computational modelling of infant movement [14], [19], [20], [21].

However, as highlighted by Silva and colleagues [19], no technological approach yet matches expert clinical judgment, and there is no quantitative gold standard, with substantial heterogeneity in extracted metrics.

Both Marker-based (MB) and Marker-less (M-*less*) systems have been explored as technological tools for automating GMA-grounded assessment of infants for CP. While multi-camera, 3D,

Received 26 September 2025; revised 17 March 2026; accepted 3 June 2026. Date of publication 17 June 2026; date of current version 13 July 2026. This work was supported in part by the National Institute on Disability, Independent Living and Rehabilitation and in part by the Administration for Community Living of the U.S. Department of Health and Human Services under Grant 90REGE0004. The review of this article was arranged by Editor Paolo Bonato. *(D. Balta and I. G. Porco contributed equally to this work.) (Corresponding author: D. Balta.)*

D. Balta and A. Cereatti are with the Politecnico di Torino, 10129 Torino, Italy (e-mail: diletta.balta@polito.it).

I. G. Porco and U. Della Croce are with the University of Sassari, 07100 Sassari, Italy.

H. Hoang, P. S. Lum, and M. M. Schladen are with the Catholic University of America, Washington, DC 20064 USA.

This article has supplementary downloadable material available at https://doi.org/10.1109/OJEMB.2026.3704501, provided by the authors.

Digital Object Identifier 10.1109/OJEMB.2026.3704501

MB approaches are well-established in research settings [19] they are impractical outside laboratory settings.

M-*less* systems, particularly single-camera approaches, offer greater accessibility and preserve natural behaviour [19] but most reported studies rely on 2D video analysis in controlled settings [15], [22], [23], [24].

In more variable clinical or home environments, depth information could improve accuracy. RGB-D systems integrating video and depth data represent a potential low-cost, compact solution suitable for such contexts [25].

The potential of M-*less* techniques is suggested by CP studies of motor development in twins during the first year after birth. Spittle and colleagues [26] showed that twins discordant for CP can display subtle motor differences as early as 12 weeks. In a home-based environment, twin studies offer a unique opportunity to observe and compare developmental trajectories while controlling many environmental confounding factors [27].

This study has two main objectives: (*i*) to adapt our previously published M-*less* protocol [28] to be more responsive to the challenges of minimally structured home video data collection, (*ii*) to preliminarily verify the hypothesis that existing metrics as derived by GMA could reveal deviations of the AR infant from his TD twin in directions consistent with prior MB studies.

This exploratory case study leverages the unique condition of twins with divergent health profiles. The goal is not to generalize findings or automate GMA, but to examine whether GMA-informed kinematic metrics preserve discriminative power when applied to infants in naturalistic, home-based settings.

II. Materials and Methods

The movement patterns of a pair of males, fraternal twins, 38.3 weeks gestation, were monitored from four to eleven months of age. One twin was TD while the other experienced Hypoxic-Ischemic Encephalopathy (HIE) at birth, demonstrated diffuse white matter and basal ganglia injury on magnetic resonance imaging (MRI), and was diagnosed AR for global developmental delay, as well as CP. An RGB-D camera (Intel RealSense D435, fs = 30 fps) was serially positioned to face each infant, placed in his baby seat at home. Video recordings of up to three minutes for each twin were captured at seven time points, spaced between 15 and 30 days apart.

The study was approved by the Institutional Review Boards of The Catholic University of America (protocol #20-0060) and Children's National Hospital (protocol #00011884). Written informed consent was obtained from the infants' parents.

The M-*less* procedure for estimating the 3D coordinates of the upper limb points of interest (PoI) was adapted from the protocol described by Balta and colleagues [28] which implemented DeepLabCut (DLC [29] - a pre-trained convolutional neural network requiring a transfer learning phase with a specialized training set based on k-means algorithm to tune the network's hyperparameters) to extract 2D PoI coordinates from RGB images.

Two critical factors may limit the routine use of the original protocol both in the clinic and at home:

1) The transfer learning phase of DLC is highly time-consuming, as it requires manual labeling of PoIs in 10% of video frames [30], selected using k-means clustering [29]. This algorithm often yields multiple similar postures, extending labeling time without adding meaningful information.
2) The reconstruction of infant movements can be affected by unintended shifts of the camera or seat, which introduce motion artifacts and may lead to misinterpretations of motor behavior.

In this work, the first limitation was addressed by refining the k-means–based training set construction through the removal of non-representative frames (e.g., when the infant was not fully visible), as well as redundant or incomplete poses, thereby reducing both training set size and labeling time.

The second limitation was addressed by creating a trunk-centered local coordinate system, CS_{Infant}, as proposed in [31], to express 3D PoI positions relative to CS_{Infant} (Fig. 1(b)) thus minimizing the effects of accidental camera or seat motion.

As in [28], after transfer learning, the 2D PoI coordinates estimated with DLC were combined with the corresponding depth data, to reconstruct 3D positions of upper-limb PoIs: left and right shoulders (LS and RS), elbows (LE and RE), wrists (LW and RW), and umbilicus (navel – N) (Fig. 1(a)). The resulting 3D trajectories were referred to CS_{Infant} and low pass filtered. The accuracy and reliability of this M-*less* 3D reconstruction methodology was previously validated through controlled experiments on infant dolls and real infant subjects [30], [32].

Additional details on the training set refinement, reference system transformation, and accuracy evaluation compared with our previous method are provided in the Supplementary Materials.

A. Metrics Estimation

This study applies GMA-derived metrics taken from the literature to 3D PoI trajectories of twin infants recorded at home, aiming to assess whether these measures can distinguish the AR twin from his TD brother in a natural setting. No clinical GMA was performed, and metrics were not correlated with specific clinical observations.

Variability and deviation from baseline were assessed through the area where wrist trajectories and velocities deviate from their moving averages (A_{WTdMA}, A_{WVdMA}) or from the standard deviation of these averages (A_{WTdMAsd}, A_{WVdMAsd}) [12], together with the Stereotypy Score (StS_{cJA}) [13]. Periodicity and distribution of movements were captured using the Periodicity Index for wrist trajectories and velocities (P_{WT}, P_{WV}) [12], the skewness of wrist velocities (SK_{WV}) [12], and the kurtosis of wrist acceleration (K_{WA}) [20]. Movement smoothness was quantified by the Jerk Index of wrist trajectories (J_{WT}). The range of motion of the elbow angle was also assessed (RoM_{EA}) [28]. Finally, coordination between limb movements (C_{WT}) and the average velocity of limb movements along the x, y, and z axes (WAV) were computed [20]. A description of each metric's calculation procedure is reported in Table I, while a more detailed definition and clinical relevance is reported in the Supplementary Materials. After extracting the metrics, data were divided into recordings up to 7.5 months and those from

TABLE I
METRICS ESTIMATION AND CLINICAL INTERPRETATION

METRIC	DEFINITION	CLINICAL INTERPRETATION		REFERENCE ARTICLE
A_{WTdMA}	Area where the 3D wrist's trajectory deviates from the moving average, adjusted for the duration of the moving average window (2s). Final value calculated as average of sums of areas computed for each direction of the right and left wrists.	Diversity and variability of movement	↓ ⇒ Chaotic movements ↑ ⇒ Fluid and congruent movements	[12], [28]
A_{WVdMA}	Area where the 3D wrist's velocity profile deviates from the moving average, adjusted for the duration of the moving average window (2s). Final value calculated as A_{WTdMA}.	Diversity and variability of movement	↓ ⇒ Chaotic movements ↑ ⇒ Fluid and congruent movements	
$A_{WTdMAsd}$	Area where 3D wrist's trajectory deviates from the standard deviation of the moving average, adjusted for the duration of deviation (normalization specifics not provided by reference work). Final value calculated as A_{WTdMA}.	Diversity and variability of movement	↓ ⇒ Poor-repertoire ↑ ⇒ Multi-facetted movements	
$A_{WVdMAsd}$	Area where 3D wrist's velocity profile deviates from the standard deviation of the moving average, adjusted for the duration of deviation (normalization specifics not provided by reference work). Final value calculated as AWTdMA.	Diversity and variability of movement	↓ ⇒ Cramped ↑ ⇒ Fidgety movements	
P_{WT}	Number of intersections of 3D wrist's trajectory with three horizontal lines each calculated as the arithmetic mean of one third of the entire signal. Final value calculated as average between sums of index calculated for each direction per wrist.	Unpredictability and complexity of movement	↑ ⇒ Poor-repertoire ↓ ⇒ Fidgety movements	
P_{WV}	Same as PWT but calculated on speed profiles.	Unpredictability and complexity of movement	↑ ⇒ Cramped or chaotic movements ↓ ⇒ Fidgety movements	
SK_{WV}	Skewness of the norm of wrist's speed profile. Final value calculated as average skewness of left and right wrist.	Presence of unusually high velocity movements	↑ ⇒ Cramped, spastic movements ↓ ⇒ Slow, small in amplitude movements	
RoM_{EA}	Range of motion of elbow angle formed by the forearm and the upper arm. Final value calculated as average between left and right range of motion.	Evaluation of range of motion	↑ ⇒Wider movements ↓ ⇒ Less extensive movements	[28]
$StSc_{JA}$	Application of Dynamic Time Warping (DTW) to calculate a similarity score on elbow (flexion/extension angle) and shoulder (abduction/adduction and elevation angle) angles. The DTW is applied only on segments of signal with angular velocity always higher than 5% of max velocity and at least once higher than 20% of max velocity. The similarity scores from different joints are combined in a similarity function and the final index is the maximum of the moving average of the similarity function.	Lack of variation in movements	↑ ⇒ Stereotypical and monotonous movements ↓ ⇒ Movements which differ for speed and amplitude	[13]
J_{WT}	Integration of the square of wrist's jerk magnitude (rate of change of the norm of acceleration) over time, normalized by tangential velocity, only during "active periods" (defined as times when the average velocity exceeds the max velocity by 5% for at least one wrist). Final value calculated as average jerk index of left and right wrist.	Steadiness/ smoothness of the movements	↑ ⇒ Unsteady movements ↓ ⇒ Smooth movements	[20]
K_{WA}	Kurtosis of the norm of wrist's acceleration, calculated on the active periods (defined as for JWT). The final value is calculated as the average kurtosis of the left and right wrist.	Presence of intermittent (burst-like) movements	↑ ⇒ Intermittent movements ↓ ⇒ More continuous movements	
C_{WT}	Correlation between wrists velocities, calculated as cross-correlations at zero-time lag between tangential wrists velocities on the active periods (defined as for JWT).	Similarity of the two arms movements	↑ ⇒ Less variability in movements ↓ ⇒ More variability in movements	
WAV	Wrist's instantaneous 3D tangential velocity (V) averaged over time. Final value calculated as average between left and right wrist's average velocity.	Overall activity	↓ ⇒ Less active ↑ ⇒ More active	

The following metrics are reported: 1) $\mathbf{A_{WTdMA}}$: Area where the 3D wrist's trajectory deviates from the moving average; 2) $\mathbf{A_{WVdMA}}$: Area where the 3D wrist's velocity profile deviates from the moving average; 3) $\mathbf{A_{WTdMAsd}}$: Area where 3D wrist's trajectory deviates from the standard deviation of the moving average; 4) $\mathbf{A_{WVdMAsd}}$: Area where 3D wrist's velocity profile deviates from the standard deviation of the moving average; 5) $\mathbf{P_{WT}}$: Periodicity Index calculated on wrists trajectories; 6) $\mathbf{P_{WV}}$: Periodicity Index calculated on wrist velocities; 7) $\mathbf{SK_{WV}}$: Skewness calculated on wrists velocities; 8) $\mathbf{RoM_{EA}}$: Range of motion of elbow angle; 9) $\mathbf{StSc_{JA}}$: Stereotypy score calculated on elbow and shoulder's angles; 10) $\mathbf{J_{WT}}$:Jerk Index calculated on wrists' acceleration; 11) $\mathbf{K_{WA}}$:Kurtosis calculated on wrists' acceleration; 12) $\mathbf{C_{WT}}$: Cross correlation between wrists velocities; 13) **WAV**: Average wrists velocity. For each metric in the second column a brief description of the calculation procedure is reported, while in the third column is reported the clinical meaning given by the reference article (citation reported in column 5). The fourth column interprets each metric by indicating what higher or lower values correspond to in terms of movement characteristics: the arrows show the relationship of metric values to movement patterns, while the color denotes developmental characteristics, with red arrows indicating AR characteristics and green arrows indicating TD characteristics.

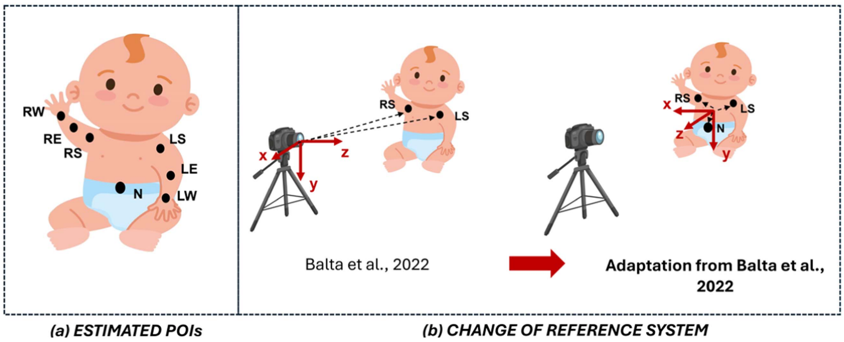

Fig. 1. (a) PoIs tracked in this study. (b) On the left side of the Fig. the coordinate system used in [28] is represented, while on the right side the adaptation used in this work is represented.

TABLE II
COMPARISON BETWEEN THE PREVIOUS METHOD [28] AND THE PROPOSED METHOD

	Previous method		Proposed method	
Training set size (frames)	536		235	
Labeling time (hours)	7.4		3.2	
FA length (mm) Ref = 95 mm	MEAN ± SD	MAE	MEAN ± SD	MAE
	113 ± 10	18	97 ± 10	2
UA length (mm) Ref = 119 mm	MEAN ± SD	MAE	MEAN ± SD	MAE
	103 ± 8	16	108 ± 5	11

The following metrics for the original and the proposed method are reported: 1) training set length; 2) time required to manually label the PoI; 3) FA and UA lengths estimations; 4) relevant errors in FA and UA lengths estimations.

8 months onward, based on qualitative video observations, to aid interpretation. This distinction was necessary because the selected metrics were developed for spontaneous movements in 3–5-month-old infants. From 7.5 months onward, the TD infant showed intentional movements, potentially altering patterns compared to those described for younger infants.

III. Results

Table II reports the results of the procedure described in the Supplementary Materials for estimating the accuracy of the proposed approach compared to the original method [28] in terms of: number of frames in the training set, time required for manual labeling, estimated lengths of forearm (FA) and upper arm (UA) in terms of mean and standard deviation (SD) and errors (in terms of Mean Absolute Error - MAE) in UA and FA lengths estimations. Table II shows an improvement in the accuracy estimate of both FA and UA lengths with respect to our previously published method [28] of about 88% and 21% respectively, and a reduction of PoI labelling by 44% compared to the original method (536 frames vs 235 frames).

Additionally, a visual example illustrates the impact of introducing the new local coordinate system. Fig. 2 shows how accidental camera motion, while the infant remained still, affected 3D PoIs reconstruction with the original method (Fig. 2(a)) and how the proposed approach compensated for this artifact (Fig. 2(b)).

For the reasons explained in the Methods, in Fig. from 3 to 7, months from 4 to 7.5 are reported in solid line, while months from 8 to 11 in lighter shade.

Fig. 3 shows that the differences between AR and TD increased with age for both the area out of the mean and the standard deviation of wrist trajectories and velocities.

In Fig. 4, the Periodicity Index of wrist velocities from 4 to 7.5 months is on average higher in TD than in AR, whereas trajectory values are, on average, comparable between AR and TD.

Fig. 5 indicates higher wrist tangential velocity and elbow range of motion in TD compared to AR.

Fig. 6 shows that TD exhibits higher values of wrist acceleration kurtosis and wrist velocity skewness. Fig. 7 shows higher correlations among limb velocities and higher Stereotypy Scores in AR, whereas the Jerk Index is higher in TD.

For all metrics, the average number of frames analyzed per video was 5400, corresponding to approximately 180 seconds of usable recording.

IV. Discussion

The first aim of our study was to improve our previously published *M-less* protocol [28], and this was achieved by addressing two main limitations: the construction of DLC training set, highly time-consuming and often including uninformative frames, and the unintended shifts of the camera /baby seat affecting the infant's movement reconstruction. The improvement in segment length estimation of the hereby presented method compared to the original one indicate that the tracking performance benefitted from the combination of the two previously described modifications. Removing repetitive frames also increased applicability, nearly halving labeling time. Although manual labeling remains a limitation, it is crucial for improving DLC accuracy compared with commercial 2D tracking software and pretrained models, as shown in [33].

The second aim of the study was to use literature-based metrics to verify the hypothesis that the AR infant would exhibit deviations from his TD twin.

Unlike reference studies based on GMA from which quantitative metrics were selected [12], [20], [13] involving 3–5-month-old infants in a supine position, our analysis was conducted on slightly older twins seated in commercial chairs that varied across timepoints.

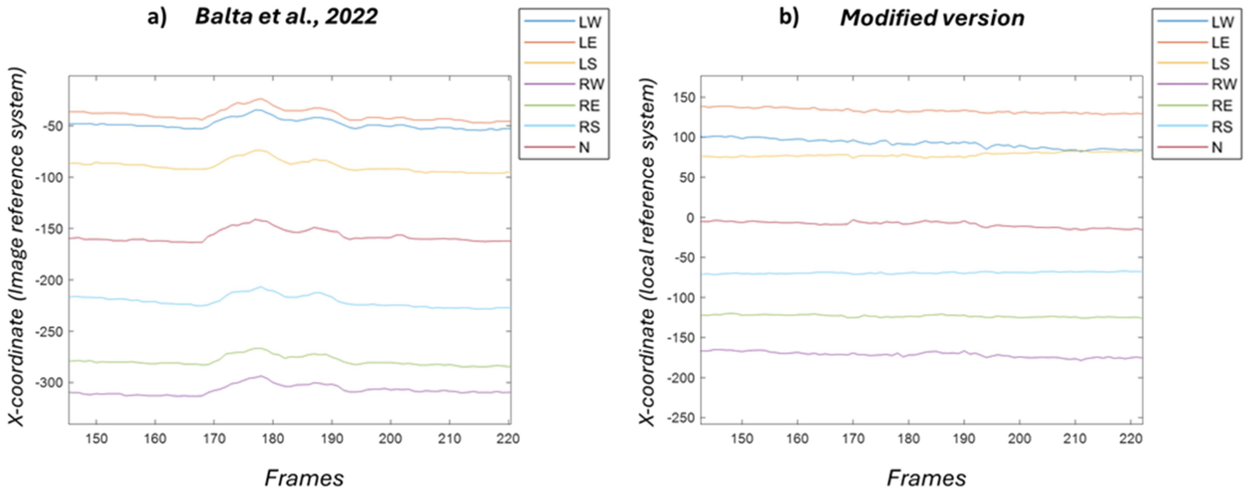

Fig. 2. Effect of an accidental camera movement on the reconstruction of 3D PoIs coordinates during data acquisition at home, while the baby was still. a) X-coordinate of each PoI referred to the image reference system during the camera motion reconstructed by the original method [28]; b) X-coordinate of each PoI referred to the infant reference system, reconstructed by the proposed version.

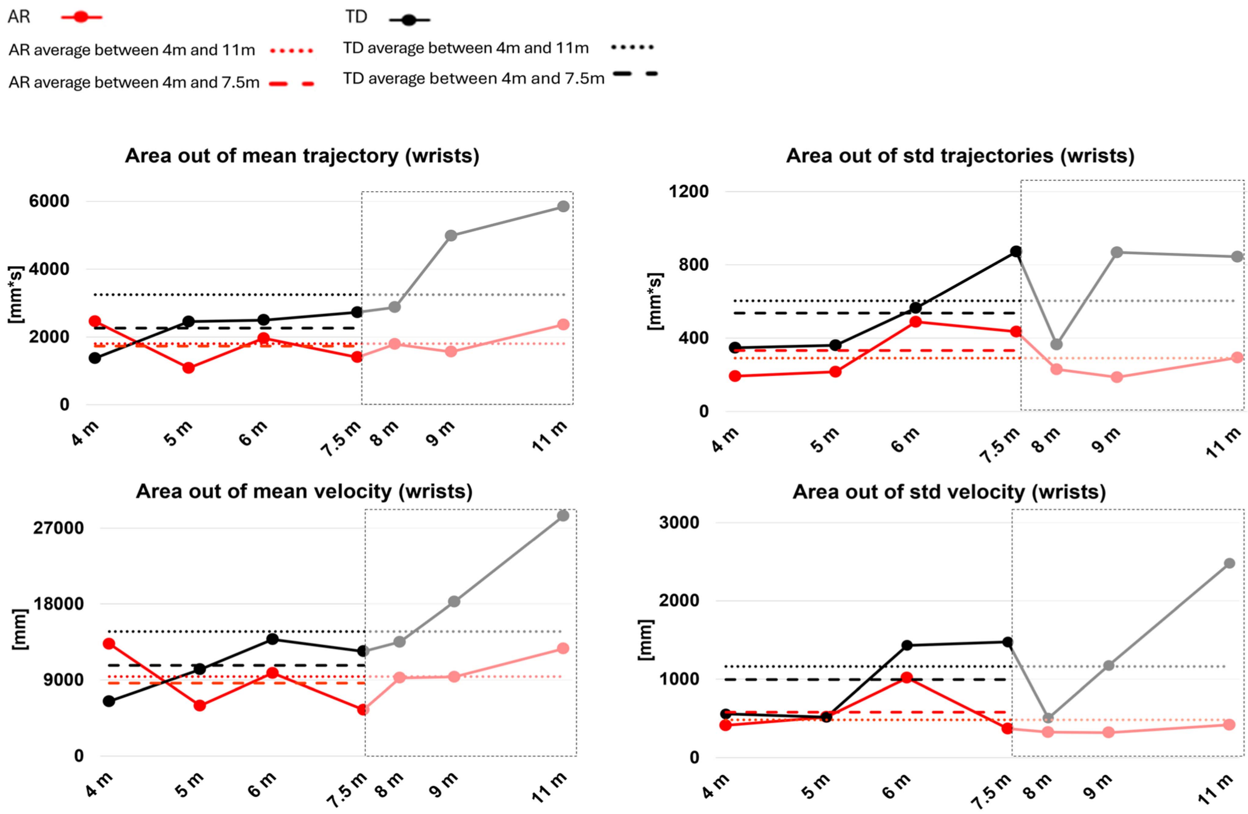

Fig. 3. Area where the wrists trajectories and velocities deviated from the moving average and area where the wrists trajectories/velocities fell outside of the standard deviation of AR (red line) and TD (black line) for each timepoint. The dashed line represents the average value from 4 to 7.5 months while the dotted line represents the average value from the 4 to 11 months. Timepoints inside the shaded box are outside the typical age range analyzed in the literature.

Visual inspection performed by a human operator showed that with age, the TD child exhibited more varied and intentional movements (e.g., clapping, hitting the table, bending forward), while the AR child remained comparatively still. These qualitative observations were consistent with the trends extracted from the quantitative metrics, which are analyzed and discussed.

A. Area Out of Mean and the Standard Deviation of Wrist Trajectories and Velocities

As originally proposed in [12], higher values of these metrics correspond to greater variability in the quantified movements. The results obtained in this study are consistent with those reported in the original work.

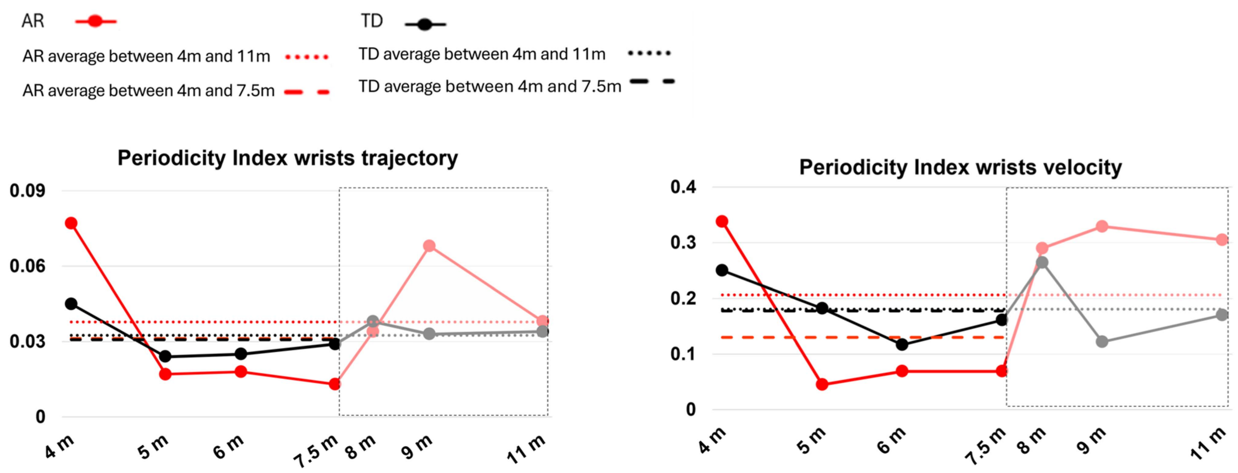

Fig. 4. Periodicity Index of wrists trajectories and velocities of AR (red line) and TD (black line) for each timepoint. The dashed line represents the average value from 4 to 7.5 months while the dotted line represents the average value from 4 to 11 months. Timepoints inside the shaded box are outside the typical age range analyzed in the literature.

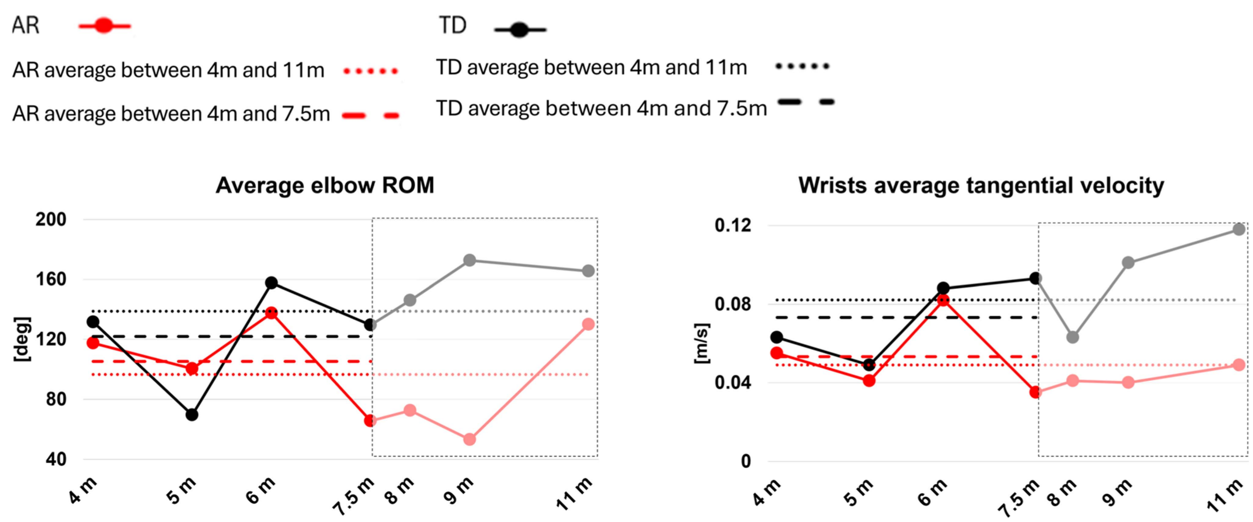

Fig. 5. Average elbow RoM and wrists average tangential velocity of AR (red line) and TD (black line) for each timepoint. The dashed line represents the average value from 4 to 7.5 months while the dotted line represents the average value from 4 to 11 months. Timepoints inside the shaded box are outside the typical age range analyzed in the literature.

B. Periodicity Index

Periodicity index showed a trend in contrast to that reported in literature [12]; therefore, we can conclude that this metric is strongly influenced by the occurrence of the repetitive, intentional, movements observed in the videos. The factor of intentionality would seem to be key to appropriate interpretation of the Periodicity Index.

C. Range of Motion of Elbow Angle

As shown in Fig. 5, this metric effectively represents the differences observed in the video recording between AR and TD, with a divergence that results in more pronounced as the infants grow.

D. Wrist Average Tangential Velocity

Values found in this study are in line with those in the reference article [20]. Interestingly, the wrist average tangential velocity shows a diverging trend between TD and AR subjects across the timepoints (Fig. 5), demonstrating that as age increases, TD shows greater activity compared to AR.

E. Kurtosis of Wrist Acceleration

In the reference article [20], wrist acceleration's kurtosis was found to be higher in the AR subject compared to the TD one. In contrast, the current study finds the opposite trend. One of the reasons could be that the kurtosis values of wrist acceleration are influenced by the presence of the repetitive and intentional movements observed in the videos. These activities were noted in the TD subject at 5, 6 and 11 months and they may lead to a more leptokurtic distribution (higher kurtosis). Such a distribution features heavier tails because these extreme movements occur more frequently than would be expected in a normal distribution.

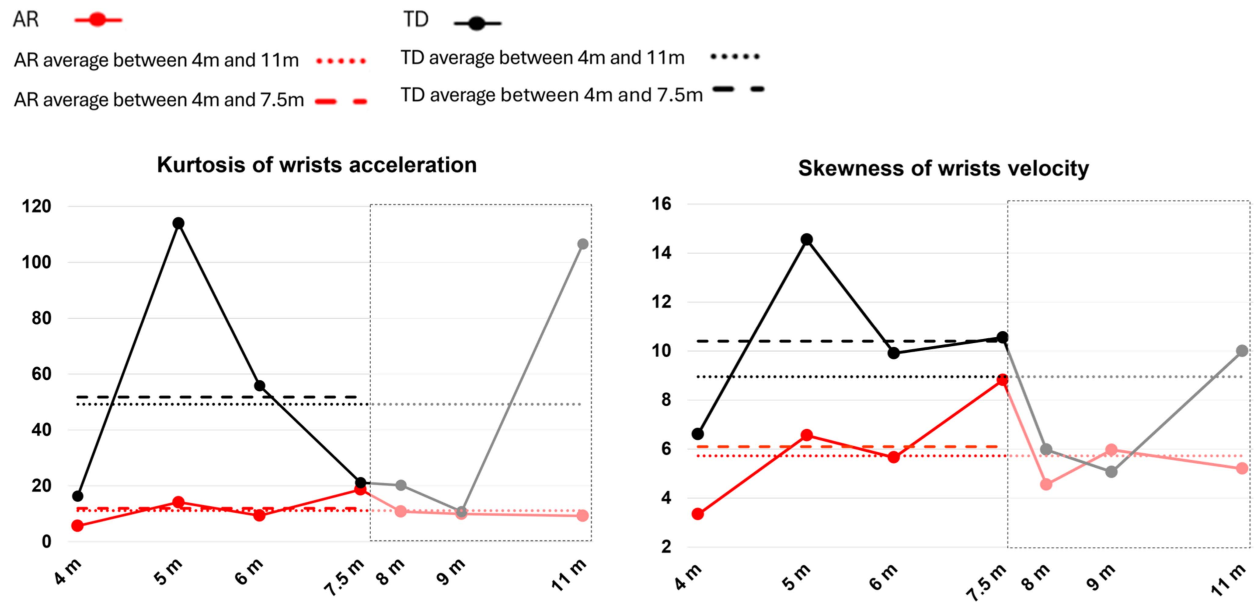

Fig. 6. Kurtosis of wrists acceleration and skewness of wrists velocities of AR (red line) and TD (black line) for each time point. The dashed line represents the average value from 4 to 7.5 months while the dotted line represents the average value from 4 to 11 months. Timepoints inside the shaded box are outside the typical age range analyzed in the literature.

F. Skewness of Wrist Velocities

As expected for both children, the skewness was positive (right-skewed) due to the dominance of movements with lower velocities. As explained in [12], for the affected newborns (such as those with certain neurological or developmental conditions), movements often involve unusually high velocities. This causes the velocity distribution to shift toward the right (positive skewness). This shift happens because high velocities are outliers compared to most slower movement velocities, thus stretching the distribution to the right. However, contrary to what is reported in [12], in our acquisition, the TD subject shows slow movements along with repetitive and intentional high-speed movements. For this reason, the velocity distribution could become positively skewed (higher skewness) reflecting the presence of higher and unequally distributed velocity values compared to those from the AR infant who shows slower and equally distributed movements (lower skewness) (Fig. 6).

G. Correlation Between Wrists Velocities

Values found in this study (Fig. 7) are in line with those in the reference article [20] with the AR subject exhibiting less variability in their movements compared to TD subject.

H. Stereotypy Score

Higher stereotypy scores indicate more repetitive and less variable movements [13], consistent with the AR twin's comparative stillness. The TD twin's lower scores reflect the broader movement repertoire expected with typical development (Fig. 7).

I. Jerk Index

There is no evident trend in the Jerk Index for either the TD or AR twin, as this measure is significantly affected by noise in the positioning of PoIs, given that it is calculated as the third derivative of the trajectories (Fig. 7). This finding is in keeping with the reference article [20] which also failed to identify any statistically significant differences between TD and AR.

To summarize, most metrics were consistent with the literature, except for the Periodicity Index, Skewness, and Kurtosis, likely affected by the TD infant's intentional movements versus the AR infant's relative stillness. Several measures (e.g., Areas, Periodicity Index, Elbow ROM, Wrist Velocity) were strongly age-dependent. In both sections of each graph, a clear divergence in their values emerges after 7.5 months, suggesting increased differentiation compared to earlier timepoints, in line with visual observations of greater motor activity in the TD child.

J. Limitations

Although the results of this study align with findings in the literature, certain limitations must be acknowledged to properly interpret the outcomes.

The identification of PoIs on RGB images depends on the visible portion of each anatomical segment, which varies with pose; for instance, the elbow may be tracked on different epicondyles depending on which side of the arm is facing the camera. This issue was partially solved by manually checking the presence of all PoI views shown in the video in the training set. The lack of strictly controlled conditions did not impair performance metrics but may explain some discrepancies. For example, seat inclination could affect movement, with a 90° angle encouraging more activity than a 45° resting position. Additionally, the presence of others may have influenced behavior, prompting intentional

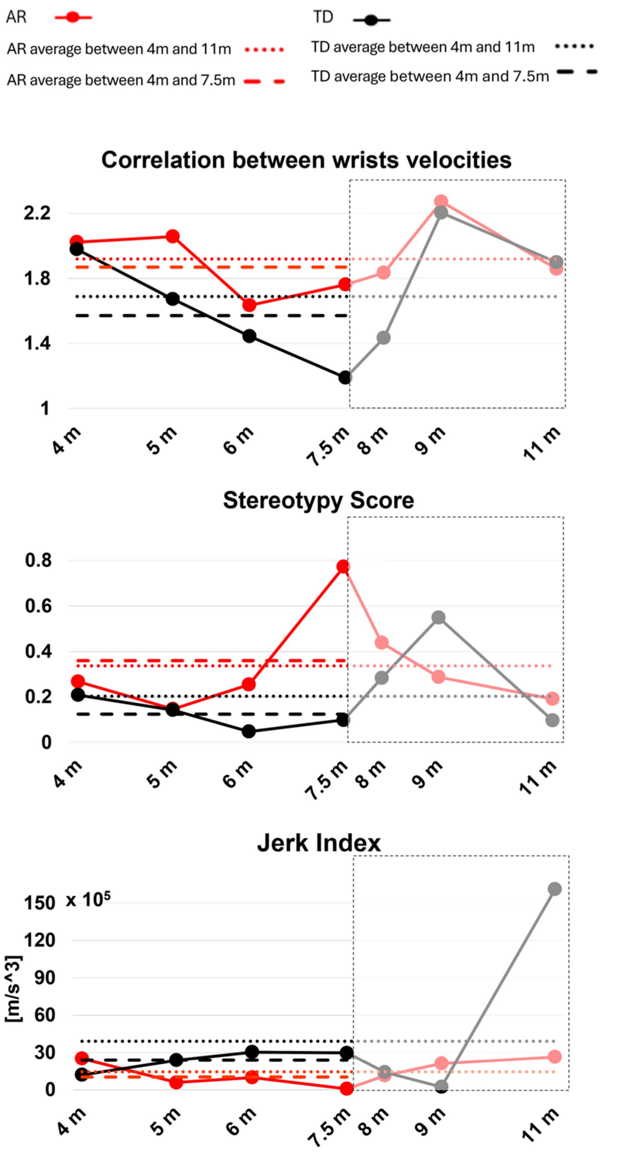

Fig. 7. Correlation between wrists velocities, Stereotypy score and jerk index of AR (red line) and TD (black line) for each timepoint. The dashed line represents the average value from 4 to 7.5 months while the dotted line represents the average value from 4 to 11 months. Timepoints inside the shaded box are outside the typical age range analyzed in the literature.

actions such as reaching or clapping. Parents were asked to limit interaction, though brief comforting occurred; segments with marked distress were excluded. While this naturalistic home setting introduces contextual variability that may affect motor patterns, the findings demonstrate methodological feasibility rather than robustness, which requires testing across multiple environments and independent validation.

V. Conclusion

The improved M-*less* method proposed in [28] compensated for motion artifacts typical of uncontrolled environments and reduced manual labeling time, enhancing clinical feasibility. Most metrics were consistent with reference studies, and effectively distinguished AR from TD infant. However, Periodicity Index, Skewness, and Kurtosis, differed from the literature, likely due to repetitive, intentional movements in the TD infant and greater stillness of the AR baby. These differences may reflect the older age of participants compared to prior studies, suggesting such metrics could be more informative at younger ages. Future work should address these limitations by extending the analysis to younger infants, further optimizing the at-home video acquisition workflow and developing new methods to recognize movement intentionality, which could provide a valuable covariate for refining the metrics explored in the present study.

Supplementary Materials

Additional information regarding the training set construction, the change of reference system and the metrics description is reported in the Supplementary Materials.

References

[1] M. Hadders-Algra, A. G. Boxum, T. Hielkema, and E. G. Hamer, "Effect of early intervention in infants at very high risk of cerebral palsy: A systematic review," *Dev. Med. Child Neurol.*, vol. 59, no. 3, pp. 246–258, 2017, doi: 10.1111/dmcn.13331.

[2] D. DeMaster et al., "Nurturing the preterm infant brain: Leveraging neuroplasticity to improve neurobehavioral outcomes," *Pediatr. Res.*, vol. 85, pp. 166–175, 2019, doi: 10.1038/s41390-018-0203-9.

[3] Arti Maria, Swati Upadhyay, and Nagaratna Vallomkonda, "Nurturing beyond the womb-early intervention practices in newborn care unit," *Indian Pediatr.*, vol. 58, no. Suppl 1, pp. 53–59, Oct. 2021.

[4] M. Oskoui, F. Coutinho, J. Dykeman, N. Jetté, and T. Pringsheim, "An update on the prevalence of cerebral palsy: A systematic review and meta-analysis," *Dev. Med. Child Neurol.*, vol. 55, no. 6, pp. 509–519, Jun. 2013, doi: 10.1111/dmcn.12080.

[5] S. McIntyre, C. Morgan, K. Walker, and I. Novak, "Cerebral palsy-don't delay," *Dev. Disabil. Res. Rev.*, vol. 17, no. 2, pp. 114–129, Nov. 2011, doi: 10.1002/ddrr.1106.

[6] C. Morgan et al., "Early intervention for children aged 0 to 2 years with or at high risk of cerebral palsy: International clinical practice guideline based on systematic reviews," *JAMA Pediatr.*, vol. 175, no. 8, pp. 846–858, Aug. 2021, doi: 10.1001/jamapediatrics.2021.0878.

[7] I. Novak et al., "Early, accurate diagnosis and early intervention in cerebral palsy: Advances in diagnosis and treatment," *JAMA Pediatr.*, vol. 171, no. 9, pp. 897–907, Sep. 2017, doi: 10.1001/jamapediatrics.2017.1689.

[8] L. Hekne, C. Montgomery, and K. Johansen, "Early access to physiotherapy for infants with cerebral palsy: A retrospective chart review," *PLoS One*, vol. 16, no. 6, Jun. 25, 2021, Art. no. e0253846, doi: 10.1371/journal.pone.0253846.

[9] B. R. Aravamuthan et al., "Uncertainties regarding cerebral palsy diagnosis opportunities to clarify the consensus definition," *Neurol. Clin. Pract.*, vol. 14, no. 6, Aug. 2024, Art. no. e200353, doi: 10.1212/CPJ.0000000000200353.

[10] L. Maitre et al., "Multi-omics signatures of the human early life exposome," *Nature Commun.*, vol. 13, no. 1, Dec. 2022, Art. no. 7024, doi: 10.1038/s41467-022-34422-2.

[11] B. Dan, P. Rosenbaum, L. Carr, M. Gough, J. Coughlan, and N. Nweke, "Proposed updated description of cerebral palsy," *Dev. Med. Child Neurol.*, vol. 67, no. 6, pp. 700–709, Jun. 2025, doi: 10.1111/dmcn.16274.

[12] C. Disselhorst-Klug, F. Heinze, N. Breitbach-Faller, T. Schmitz-Rode, and G. Rau, "Introduction of a method for quantitative evaluation of spontaneous motor activity development with age in infants," *Exp. Brain Res.*, vol. 218, no. 2, pp. 305–313, Apr. 2012, doi: 10.1007/s00221-012-3015-x.

[13] D. Karch et al., "Kinematic assessment of stereotypy in spontaneous movements in infants," *Gait Posture*, vol. 36, no. 2, pp. 307–311, Jun. 2012, doi: 10.1016/j.gaitpost.2012.03.017.

[14] L. Meinecke, N. Breitbach-Faller, C. Bartz, R. Damen, G. Rau, and C. Disselhorst-Klug, "Movement analysis in the early detection of newborns at risk for developing spasticity due to infantile cerebral palsy," *Hum. Movement Sci.*, vol. 25, no. 2, pp. 125–144, Apr. 2006, doi: 10.1016/j.humov.2005.09.012.

[15] M. Moro et al., "A markerless pipeline to analyze spontaneous movements of preterm infants," *Comput. Methods Programs Biomed.*, vol. 226, Nov. 2022, Art. no. 107119, doi: 10.1016/j.cmpb.2022.107119.

[16] S. Orlandi et al., "Detection of atypical and typical infant movements using computer-based video analysis," in *Proc. Annu. Int. Conf. IEEE Eng. Med. Biol. Soc.*, Jul. 2018, pp. 3598–3601, doi: 10.1109/EMBC.2018.8513078.

[17] H. F. Prechtl, C. Einspieler, C. Cioni, A. F. Bos, F. Ferrari, and D. Sontheimer, "An early marker for neurological deficits after perinatal brain lesions," *Lancet*, vol. 349, May 10, 1997, Art. no. 9062, doi: 10.1016/S0140-6736(96)10182-3.

[18] H. F. R. Prechtl, "Qualitative changes of spontaneous movements in fetus and preterm infant are a marker of neurological dysfunction," *Early Hum. Dev.*, vol. 23, no. 3, pp. 151–158, 1990, doi: 10.1016/0378-3782(90)90011-7.

[19] N. Silva et al., "The future of general movement assessment: The role of computer vision and machine learning – A scoping review," *Res. Dev. Disabil.*, vol. 110, Mar. 2021, Art. no. 103854, doi: 10.1016/j.ridd.2021.103854.

[20] N. Kanemaru et al., "Specific characteristics of spontaneous movements in preterm infants at term age are associated with developmental delays at age 3 years," *Dev. Med. Child Neurol.*, vol. 55, no. 8, pp. 713–721, Aug. 2013, doi: 10.1111/dmcn.12156.

[21] H. I. Shin et al., "Deep learning-based quantitative analyses of spontaneous movements and their association with early neurological development in preterm infants," *Sci. Rep.*, vol. 12, no. 1, Dec. 2022, Art. no. 3138, doi: 10.1038/s41598-022-07139-x.

[22] L. Adde, J. L. Helbostad, A. R. Jensenius, G. Taraldsen, K. H. Grunewaldt, and R. StØen, "Early prediction of cerebral palsy by computer-based video analysis of general movements: A feasibility study," *Dev. Med. Child Neurol.*, vol. 52, no. 8, pp. 773–778, Aug. 2010, doi: 10.1111/j.1469-8749.2010.03629.x.

[23] E. A. F. Ihlen et al., "Machine learning of infant spontaneous movements for the early prediction of cerebral palsy: A multi-site cohort study," *J. Clin. Med.*, vol. 9, no. 1, Jan. 2020, Art. no. 5, doi: 10.3390/jcm9010005.

[24] R. Stagni et al., "General movements automatic assessment: Methodological issues for pose estimation," *Gait Posture*, vol. 106, pp. S195–S196, 2023, doi: 10.1016/j.gaitpost.2023.07.236.

[25] C. Marcroft, A. Khan, N. D. Embleton, M. Trenell, and T. Plötz, "Movement recognition technology as a method of assessing spontaneous general movements in high risk infants," *Front Neurol.*, vol. 5, Jan. 9, 2015, Art. no. 284, doi: 10.3389/fneur.2014.00284.

[26] A. J. Spittle, C. Morgan, J. E. Olsen, I. Novak, and J. L. Y. Cheong, "Early diagnosis and treatment of cerebral palsy in children with a history of preterm birth," *Clin. Perinatol.*, vol. 45, no. 3, pp. 409–420, 2018, doi: 10.1016/j.clp.2018.05.011.

[27] C. Arpino et al., "Preterm birth and neurodevelopmental outcome: A review," *Child's Nervous Syst.*, vol. 9, pp. 1139–1149, Sep. 26, 2010, doi: 10.1007/s00381-010-1125-y.

[28] D. Balta et al., "Characterization of infants' general movements using a commercial RGB-depth sensor and a deep neural network tracking processing tool: An exploratory study," *Sensors*, vol. 22, no. 19, Oct. 2022, Art. no. 7426, doi: 10.3390/s22197426.

[29] A. Mathis et al., "DeepLabCut: Markerless pose estimation of user-defined body parts with deep learning," *Nature Neurosci.*, vol. 21, no. 9, pp. 1281–1289, Sep. 2018, doi: 10.1038/s41593-018-0209-y.

[30] D. Balta et al., "Estimating infant upper extremities motion with an RGB-D camera and markerless deep neural network tracking: A validation study," in *Proc. 44th Annu. Int. Conf. IEEE Eng. Med. Biol. Soc.*, 2022, pp. 2548–2551.

[31] D. Balta et al., "An improved method for the characterization of infants' general movements using a RGB-Depth sensor and a deep neural network tracking processing tool," in *Convegno Nazionale di Bioingegneria*. Padova, Italy: Patron Editore S.r.l., 2023. [Online]. Available: https://www.scopus.com/inward/record.uri?eid=2-s2.0-85175855904&partnerID=40&md5=93326c32421c8e66911af8223e4b7de8

[32] D. Balta et al., "Infant upper body 3D kinematics estimated using a commercial RGB-D sensor and a deep neural network tracking processing tool," in *Proc. 17th Ed. IEEE Int. Symp. Med. Meas. Appl.*, 2022, pp. 1–6.

[33] G. Panconi, S. Grasso, S. Guarducci, L. Mucchi, D. Minciacchi, and R. Bravi, "DeepLabCut custom-trained model and the refinement function for gait analysis," *Sci. Rep.*, vol. 15, no. 1, Dec. 2025, Art. no. 2364, doi: 10.1038/s41598-025-85591-1.